Journal of Thermal Analysis and Calorimetry, Vol. 94 (2008) 1, 53–57

THE EFFECT OF Co^{2+}-DOPING ON TETRA(THIOUREA)COPPER(I) CHLORIDE CRYSTALS

G. Sivakumar[1], *Md. R. Ahmed*[2], *S. Parthiban*[2], *S. P. Meenakshisundaram*[2] *and S. C. Mojumdar*[3,4*]

[1]CISL, Department of Physics, Annamalai University, Annamalai Nagar 608 002, India
[2]Department of Chemistry, Annamalai University, Annamalai Nagar 608 002, India
[3]Department of Chemical Engineering and Applied Chemistry, University of Toronto, 200 College St., Toronto, ON, M5S 3E5, Canada
[4]University of New Brunswick, Saint John, NB, E2L 4L5, Canada

Single crystals of the organometallic material tetra(thiourea)copper(I) chloride (TTCC) were grown from aqueous solution. It is interesting to observe that Co^{2+}-doping influences the efficiency of some of the physical properties of TTCC. Presence of Co^{2+} ions in the doped specimen is confirmed by energy dispersive X-ray spectroscopy (EDS) and chemical tests. FTIR studies reveal that the binding of thiourea with copper chloride occurs through sulphur. Doping results in reduction in the intensity of XRD peaks. SEM reveals that doping results in layered growth of the crystal. DSC confirms slight variations in the decomposition pattern. Mechanical stability of the doped specimen is much better than TTCC. Optical transparency is slightly enhanced by doping and a wide transmission in the visible region is observed. TTCC is non-linear optics (NLO) inactive and the second harmonic generation (SHG) efficiency is not influenced much by the added dopant.

Keywords: *cobalt, copper, doping effects, DSC, EDS, FTIR, TTCC, XRD*

Introduction

The copper thiourea compound $[Cu\{S=C(NH_2)_3\}]Cl$ is prepared with relative ease. Generally, the compounds of Cu(I) are often quite insoluble in water, however they are very soluble in aprotic solvents. Along with $[CuCl_2]^-$, tris(thiorea)copper(I) chloride [1] and tetra(thiourea)copper(I) chloride [2] are some of the few water-soluble forms of Cu(I). These Cu(I) complexes are quite stable. They do not undergo oxidation to Cu(II) or reduction to Cu metal. Many authors have investigated organometallic compounds due to their chemical, biological and environmental significance and their thermal, spectral, microscopic and many other properties have also been examined [3–22]. In recent years, some materials doped with tetrahedral Co^{2+} have been reported and it is interesting to observe excellent absorption, emission [23–27] and magnetic [28] properties. $ZnGa_2O_4$ nanocrystals exhibit strong broad luminescence bands in the visible and near infrared spectral regions [29, 30]. It has been reported [27] that Co^{2+} ions locate in the tetrahedral sites in the $ZnGa_2O_4$ nanocrystallites. Recently, we have observed that the dopant KCl occupies the interstitial positions in the crystalline matrix by HRXRD studies. The coloration mechanism, an inclusion effect is suggested [28] in the co-doped synthetic blue quartz. Further, cobalt doping enhances the catalytic properties of ferric oxide by increasing the calcination temperature [31]. The effect of cobalt oxide additions in $ZnO–Bi_2O_3$-based varistors suggested the improvement in the nonlinear properties [32]. It is seen that superconducting transition temperature (T_c) in YBCO single crystals is considerably enhanced by cobalt doping [33]. In this paper we report the effect of Co^{2+}-doping on some physical properties of TTCC since cobalt as a dopant influences the efficiency of the physical properties.

Experimental

Synthesis and crystal growth

The material was synthesized using thiourea (1.0 g thiourea in 5.0 mL hot water), copper turnings (0.20 g) and conc. HCl (1 mL)

$$Cu+4(NH_2)_2CS+HCl\rightarrow[Cu\{SC(NH_2)_2\}_4]Cl$$

The product was purified by repeated recrystallisation. The crystal growth was carried out in the presence of a small quantity ($5\cdot10^{-3}$) of $CoCl_2$ dopant in the aqueous growth medium by slow evaporation solution growth technique. At low concentrations of Co, the growth promoting effect (GPE) is much greater than that observed in the absence of

* Author for correspondence: scmojumdar@hotmail.com

1388–6150/$20.00

Akadémiai Kiadó, Budapest, Hungary
Springer, Dordrecht, The Netherlands

dopant. Bulk crystals are grown using the optimized growth parameters. The Co^{2+}-doped specimen exhibits beautiful blue tints (Fig. 1).

Methods

Microhardness measurements

Hardness is the resistance offered by a material to localized plastic deformation caused by scratching or by indentations. Vickers microhardness was evaluated for the well polished grown crystal and dominant (001) plane using Reichert 4000E Ultramicrohardness Tester.

$$\text{Microhardness number, } Hv = 1.8544\ p\ d^{-2}$$

where p is the load in kg and d is the diagonal length of indentation (mm).

Optical transmission spectra

The UV-Visible absorption spectra were recorded using Hitachi UV-Vis spectrophotometer in the spectral range 250–800 nm for all samples.

FTIR spectra

The FTIR spectra were recorded for all samples including pure TTCC on an AVATAR 330 FTIR using KBr pellet technique in the range 500–4000 cm^{-1}.

Powder XRD

Powder X-ray diffraction is useful for confirming the identity of a solid material and determining crystallinity and phase purity. The powder X-ray diffractometry (XRD) analysis was performed with a graphite monochromated CuK_α radiation. The XRD data was analysed with Rietveld method with RIETAN-2000.

Differential scanning calorimetric (DSC) studies

DSC curves were recorded using a DSC-60 Shimadzu analyzer at a heating rate of 20°C min^{-1}.

SEM and EDS

The surface morphology was observed using a JEOL JSM 5610 LV scanning electron microscope with an accelerating voltage of 20 kV, at high vacuum mode and secondary electron image (SEI). In the SEM, the image is formed and presented by a very fine electron beam, which is focused on the surface of the specimen. At any given moment, the specimen is bombarded with electrons over a very small area.

Energy dispersive X-ray spectroscopy (EDS) is a chemical microanalysis technique performed in conjunction with a scanning electron microscope (SEM). The technique utilizes X-rays that are emitted from the sample during bombardment by the electron beam to characterize the elemental composition of the analyzed volume. Features or phases as small as 1 μm can be analyzed. When the sample is bombarded by the electron beam of SEM, electrons are ejected from the atoms comprising the sample's surface. A resulting electron vacancy is filled by an electron from a higher shell, and an X-ray is emitted to balance the energy difference between the two electrons. The EDS X-ray detector measures the number of emitted X-rays *vs*. their energy. The energy of the X-ray is characteristic of the element from which the X-ray was emitted. A spectrum of the energy versus relative counts of the detected X-rays is obtained and evaluated for qualitative and quantitative determinations of the elements present in the sampled volume. This method can detect elements from sodium upward in the periodic table.

Kurtz powder second harmonic generation (SHG) measurements

The SHG test on the crystals was performed by the Kurtz powder SHG method [34]. An Nd:YAG laser with modulated radiation of 1064 nm was used as the optical source and directed on the powdered sample through a filter. The grown crystals were ground to a uniform particle size of 125–150 mm and then packed in a micro-capillary of uniform bore and exposed to laser radiation.

Results and discussion

Microhardness test

The polished face of pure TTCC and doped TTCC were subjected to static indentation tests at room temperature. Depending upon the microhardness, load for crystal have been evaluated and loads of different magnitude (25, 50, 75, 100 and 125 g) were applied on plane of crystals for a fixed interval of time. For each load, several indentations were made and the average value of the diagonal length was used to calculate the microhardness. A plot drawn between the hardness value and the corresponding loads of TTCC and doped crystals are shown in Figs 2a and b, respectively. Hardness is found to increase as the load is increased and it attains a constant value for the load of 75 g for TTCC and 100 g for doped TTCC. When indentation load of 100 g for pure TTCC and 125 g for Co–TTCC was applied, cracks were indicated on the crystal surface around the indenter. The better mechanical properties of TTCC imply

Fig. 1 Photographs of a – pure TTCC and b – Co^{2+}-doped TTCC

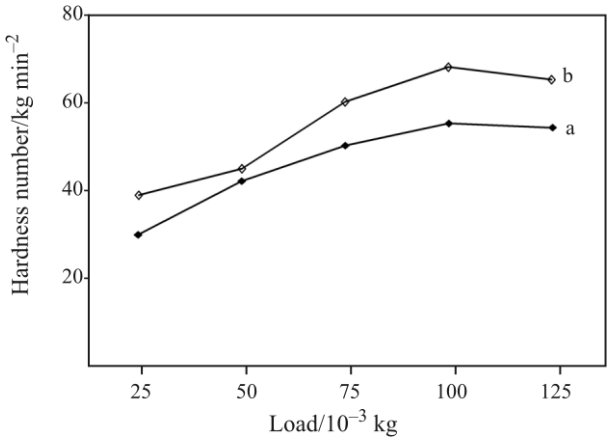

Fig. 2 Microhardness graphs of a – pure TTCC and b – Co^{2+}-doped TTCC

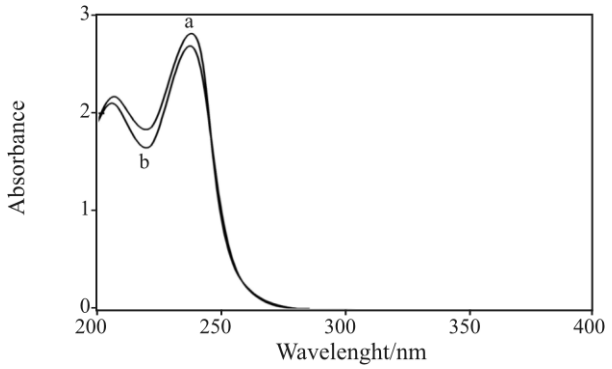

Fig. 3 UV-Vis spectra of a – pure TTCC and b – Co^{2+}-doped TTCC

that Co^{2+}-doped TTCC crystal is a good engineering material for device fabrication.

UV-Vis studies

It appears from UV spectrum that doping by cobalt does not affect the perfection of crystals. Also, it slightly enhances the percentage of transmittance (Fig. 3). A wide transmission in the visible region is observed.

FTIR spectra

The FTIR spectra were recorded for pure TTCC and Co^{2+}-doped TTCC using KBr pellet technique. The characteristic vibrational frequencies of pure TTCC

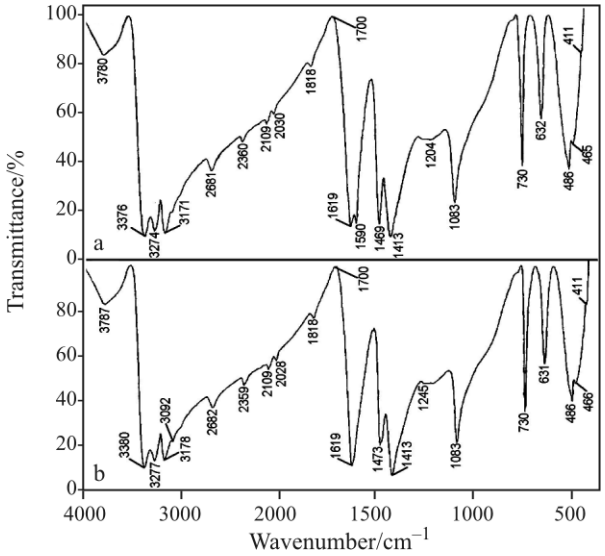

Fig. 4 FTIR spectra of a – pure TTCC and b – Co^{2+}-doped TTCC

and dopant added TTCC are very similar. The symmetric and asymmetric C–S stretching vibrations at 740 and 1417 cm^{-1} of thiourea are shifted to lower frequencies in the FTIR spectra [35]. The band ~1425 cm^{-1} is assigned to N–C–N stretching vibration (Fig. 4). The other characteristic vibrational frequencies are assigned elsewhere [2]. The characteristic vibrational frequencies of doped specimen are very similar.

Powder XRD

XRD patterns of Co^{2+}-doped TTCC crystals are compared with that of pure TTCC crystals. The X-ray study

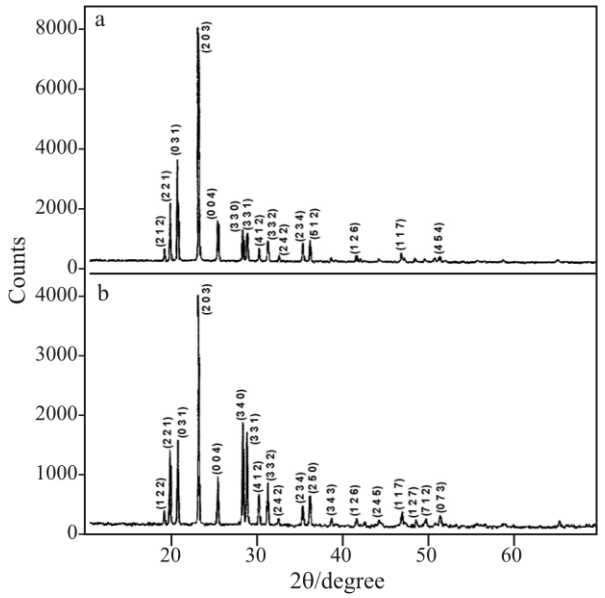

Fig. 5 Powder XRD patterns of a – pure TTCC and b – Co^{2+}-doped TTCC

revealed that there is a slight reduction in intensity and the structures of doped crystals (10 mol%) are slightly distorted compared to the pure TTCC crystal. This may be attributed to strains on the lattice [36]. The sharp well defined Bragg's peaks at specific 2θ angle confirm the crystallinity of the specimen (Fig. 5). There is not much of variation in the cell parameter values of the doped specimen. This is quite expected as the dopant is added in small concentration ($5 \cdot 10^{-3}$ M L^{-1}). The calculated lattice parameter values are $a=b=13.4015$ Å, $c=13.8492$ Å, $V=2487.330$ Å^3, $\alpha=\beta=\gamma=90°$ and the crystal belongs to tetragonal system with the space group $P4_12_12$, which is in good agreement with the reported values [37].

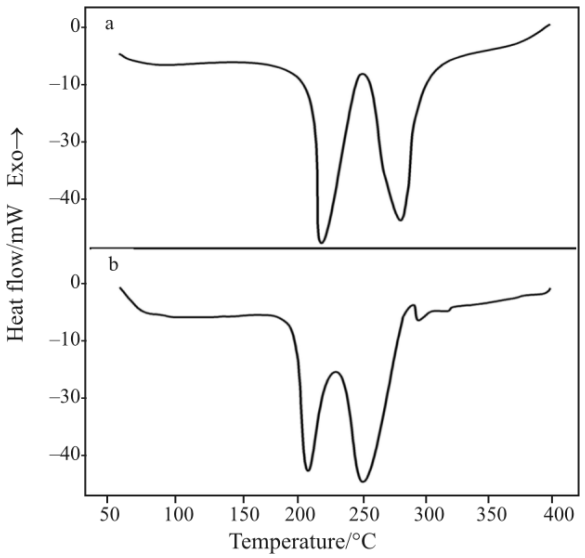

Fig. 6 DSC curves of: a – pure TTCC and b – Co^{2+}-doped TTCC

DSC studies

In both TTCC and Co^{2+}-doped TTCC crystals two intense endothermic peaks were observed. Second endothermic peak at 230°C for TTCC and at 249°C for Co^{2+}-TTCC are due to decomposition (Fig. 6). The DSC results reveal that there is no water of hydration and the mechanical stability increases in the presence of dopant Co^{2+}.

Scanning electron microscopy (SEM)

Figure 7 shows the SEM micrographs of grown TTCC and doped TTCC crystals. Both have well developed morphology with several habit faces. The morphology of Co^{2+}-doped TTCC crystals is different from that of pure TTCC. Microscopical examination of the habit faces reveals the presence of spreading micro-layer. Careful examination of the surface of the crystals under the SEM shows of parallel (slip) lines.

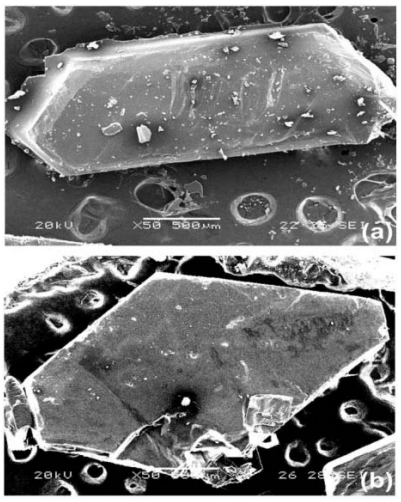

Fig. 7 SEM micrographs of: a – pure TTCC and b – Co^{2+}-doped TTCC

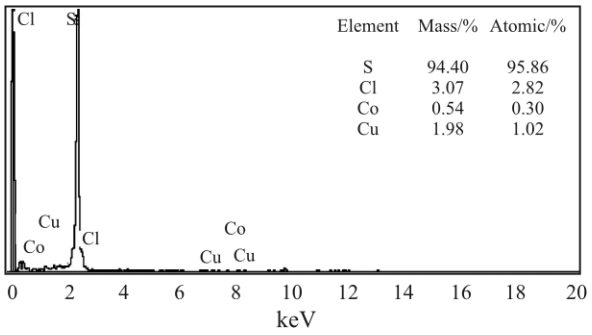

Fig. 8 EDS spectrum of Co^{2+}-doped TTCC crystal

This indicates that the atomic planes within the crystal have sheared with respect to one another resulting in surface steps. Non uniform surface of the doped specimen could be due to the inclusion of Co^{2+}.

EDS

Doped TTCC crystals were subjected to EDS analysis in order to confirm the presence of sulphur and cobalt. Incorporation of Co^{2+} in the doped specimen is confirmed from Fig. 8. Further, the presence of the cobalt in the doped specimen is confirmed by testing with NH_4Cl, NH_4OH and potassium ferricyanide solution. It is interesting to observe the incorporation of chloride ions in the crystalline matrix. Davey and Mullin [38] have shown that $NH_4H_2PO_4$ (ADP) crystals grown in the presence of $CrCl_3 \cdot 6H_2O$ contain both Cr^{3+} and Cl^- ions. More inclusions are observed when the dopant concentration is increased.

SHG test

In order to confirm the NLO property, the as grown crystals were subjected to NLO test. No doubling of fre-

quency and the absence of emission of green light at 532 nm confirms the absence of NLO activity in both TTCC and doped TTCC. It appears that the doping has no influence on the NLO property of this crystal.

Conclusions

The incorporation of Co^{2+} in the crystalline matrix of TTCC crystals is well confirmed by EDS and chemical tests. Small quantity addition of Co^{2+} in the aqueous growth medium facilitates the growth process. SEM reveals the varied morphology in the presence of the dopant. Doping has no effect on the NLO property. The Co^{2+}-doping influences the mechanical stability and percentage transmittance. Doping of Co^{2+} in the crystalline matrix of TTCC is advantageous in the crystallization process.

References

1 K. Jonson and J. W. Steed, J. Chem. Soc., Dalton Trans., (1998) 2601.
2 M. Dhandapani, M. A. Kandhaswamy and V. Srinivasan, Cryst. Res. Technol., 40 (2005) 805.
3 J. S. Skoršepa, K. Györyová and M. Melník, J. Thermal Anal., 44 (1995) 169.
4 E. Jóna, E. Rudinská, M. Sapietová, G. Rudinská and S. C. Mojumdar, J. Therm. Anal. Cal., 90 (2007) 687.
5 K. G. Varshney, A. Agrawal and S. C. Mojumdar, J. Therm. Anal. Cal., 90 (2007) 721.
6 S. C. Mojumdar, M. Sain, R. Prasad, L. Sun and J. E. S. Venart, J. Therm. Anal. Cal., 90 (2007) 653.
7 H. S. Rathore, G. Varshney, S. C. Mojumdar and M. T. Saleh, J. Therm. Anal. Cal., 90 (2007) 681.
8 E. Jona, M. Sapietová, V. Pavlík, G. Rudinská, D. Ondrušová, M. Pajtášová and S. C. Mojumdar, Res. J. Chem. Environ., 11 (2007) 23.
9 K. G. Varshney, A. Agrawal and S. C. Mojumdar, J. Therm. Anal. Cal., 90 (2007) 731.
10 K. G. Varshney, V. Jain, A. Agrawal and S. C. Mojumdar, J. Therm. Anal. Cal., 86 (2006) 609.
11 M. T. Saleh, S. C. Mojumdar and M. Lamoureux, Res. J. Chem. Environ., 10 (2006) 14.
12 R. A. Porob, S. Z. Khan, S. C. Mojumdar and V. M. S. Verenkar, J. Therm. Anal. Cal., 86 (2006) 605.
13 S. C. Mojumdar, K. G. Varshney and A. Agrawal, Res. J. Chem. Environ., 10 (2006) 89.
14 B. Borah and J. L. Wood, Can. J. Chem., 50 (1976) 2470.
15 S. C. Mojumdar, G. Madhurambal and M. T. Saleh, J. Therm. Anal. Cal., 81 (2005) 205.
16 E. Jóna, M. Kubranová, P. Šimon and J. Mroziński, J. Therm. Anal. Cal., 46 (1996) 1325.
17 S. C. Mojumdar, L. Martiška, D. Valigura and M. Melník, J. Therm. Anal. Cal., 81 (2005) 243.
18 D. Czakis-Sulikowska, A. Czylkowska and A. Malinowska, J. Therm. Anal. Cal., 65 (2001) 505.
19 S. C. Mojumdar, J. Miklovic, A. Krutošíková, D. Valigura and J. M. Stewart, J. Therm. Anal. Cal., 81 (2005) 211.
20 G. Madhurambal, S. C. Mojumdar, S. Hariharan and P. Ramasamy, J. Therm. Anal. Cal., 78 (2004) 125.
21 E. A. Ukraintseva, V. A. Logvinenko, D. V. Soldatov and T. A. Chingina, J. Therm. Anal. Cal., 75 (2004) 337.
22 S. C. Mojumdar, J. Therm. Anal. Cal., 64 (2001) 629.
23 N. V. Kuleshov, V. P. Mikhailov, V. G. Scherbitsky, P. V. Prokoshin and K. V. Yumashev, J. Lumin., 55 (1993) 265.
24 K. V. Yumashev, Appl., Opt., 38 (1999) 6343.
25 M. B. Camargo, R. D. Stultz, M. Birnbaum and M. Kokta, Opt. Lett., 20 (1995) 339.
26 I. A. Denisov, M. L. Demchuk, N. V. Kuleshov and K. V. Yumashec, Appl. Phys. Lett., 77 (2000) 2455.
27 X. L. Duan, D. R. Yuan, L. H. Wang, F. P. Yu, X. F. Cheng, Z. Q. Liu and S. S. Yan, J. Cryst. Growth, 296 (2006) 234.
28 X. Mao, F. Xu, J. Tang, W. Gao, S. Li and Y. Du, J. Magn. Magn. Mater., 288 (2005) 106.
29 T. Abritta and F. H. Blak, J. Lumin., 48–49 (1991) 558.
30 L. P. Sosman, A. D. Tavares and T. Abritta, J. Phys. D: Appl. Phys., 33 (2000) L19.
31 W. M. Shaheen, Mater. Chem. Phys., 101 (2007) 182.
32 W. Onreabroy and N. Sirikulrat, Mater. Sci. Eng., B130 (2006) 108.
33 S. Elizabeth, A. Anand, S. V. Bhat, S. V. Subramanyam and H. L. Bhat, Solid State Commun., 109 (1999) 333.
34 S. K. Kurtz and J. J. Perry, J. Appl. Phys., 39 (1968) 3798.
35 J. Ramajothi, S. Dhanuskodi and K. Nagarajan, Cryst. Res. Technol., 39 (2004) 414.
36 M. Rak, N. N. Eremin, J. A. Eremina, V. A. Kuznetsov, T. M. Okhrimenko, N. G. Furmanova and E. P. Efremova, J. Cryst. Growth, 273 (2005) 577.
37 S. Lakshimi, M. A. Sridhar, J. S. Prasad, V. Srinivasan, M. A. Kandhaswamy and M. Dhandapani, Anal. Sci., 19 (2003) 19.
38 R. J. Davey and J. W. Mullin, J. Cryst. Growth, 23 (1974) 89.

DOI: 10.1007/s10973-008-9187-8